Optical properties of linear-chain mercury compounds*

Dale L. Peebles, C. K. Chiang, Marshall J. Cohen, and A. J. Heeger
Department of Physics and Laboratory for Research on the Structure of Matter, University of Pennsylvania, Philadelphia, Pennsylvania 19174

N. D. Miro and A. G. MacDiarmid
Department of Chemistry and Laboratory for Research on the Structure of Matter, University of Pennsylvania, Philadelphia, Pennsylvania 19174

(Received 14 January 1977; revised manuscript received 23 February 1977)

Polarized reflectance studies from single-crystal faces of the anisotropic Hg-chain conductor $Hg_{2.86}$ AsF_6 are presented. The results indicate metallic behavior for electronic excitations along the chains (in the $\vec{a}$-$\vec{b}$ plane) with free-electron Drude theory giving a satisfactory initial description of the data. The plasma frequency is found to be $\hbar\omega_p = 4.8$ eV and combined with the electron density yields a free-electron optical mass. The implied optical conductivity in the a-b plane at room temperature is $\sigma_{opt} = (4\pi)^{-1}\omega_p^2\tau \simeq 10^4$ $(\Omega\,\mathrm{cm})^{-1}$ in good agreement with the measured dc value. Normal-incidence studies of reflectance from crystal faces at an angle with the a-b plane are analyzed to provide a complete description of the complex dielectric tensor in the spectral range from 0.5 to 4.2 eV.

I. INTRODUCTION

A new class of anisotropic conductors containing metallic chains of mercury atoms has recently been reported.[1,2] Cutforth *et al.*[1] showed that the compound with nominal formula $Hg_3(AsF_6)$ consists of metallically bonded polymercury cations in a tetragonal lattice consisting of an array of $(AsF_6)^-$ anions. The mercury chains are situated in nonintersecting channels along the $\vec{a}$ and $\vec{b}$ axes of the tetragonal lattice.[2] There are no chains along $\vec{c}$. The Hg-Hg distance within a chain was inferred from observations of diffuse scattering streaks indicative of a periodicity of 2.64 Å.[2] Brown *et al.*[2] assumed these streaks arose from the polymercury chains with Hg-Hg distance of 2.64 Å, but with no phase coherence between chains. Since the lattice constant is $a=b=7.54$ Å, the empirical structural formula is $Hg_{2.86}AsF_6$ implying that the mercury atoms in a chain are incommensurate with the unit cell of the tetragonal lattice. This remarkable incommensurate chain-like structure and the implied mixed valence of the mercury atoms are suggestive of features found in the one-dimensional conductors tetrathiafulvalene-tetracyanoquinodimethane[3,4] (TTF-TCNQ) and potassium cyano-platinide[3,4] (KCP). Moreover, the structure of interpenetrating metal atom chains is reminiscent of the A-15 high-temperature superconductors. Accordingly we have initiated a broad study of the electronic properties of this novel class of anisotropic metals.

In this paper we report on optical reflectance studies in the visible and near infrared (0.5–4.2 eV; 4000–34 000 cm^{-1}) carried out on large single crystals of $Hg_{2.86}AsF_6$. The Drude-like optical reflectance results confirm the metallic nature of the compound along the chain directions. A study of the normal-incidence reflectance on several crystal faces provides detailed information on the anisotropic dielectric function with the particular result that for light polarized perpendicular to the chains, ϵ_c is constant throughout the experimental range with no sign of metallic behavior.

The experimental methods are described in Sec. II including details on crystal growth and handling for the optical measurements. The reflectance data are presented in Sec. III. The results are analyzed in Sec. IV in terms of normal-incidence reflectance for an anisotropic medium in which $\epsilon_{ab}(\omega)$ is the Drude dielectric function characteristic of simple metallic behavior and ϵ_c is constant (ϵ_{ab} refers to light polarized in the $\vec{a}$-$\vec{b}$ plane defined by directions of the two sets of Hg chains; ϵ_c refers to light polarized along $\vec{c}$ and perpendicular to both sets of chains):

$$\epsilon_{ab}(\omega) = \epsilon_\infty - \omega_p^2/(\omega^2 + i\omega/\tau)\,, \tag{1a}$$

$$\epsilon_c(\omega) = \epsilon_\infty\,, \tag{1b}$$

where ϵ_∞ is the core dielectric constant, $\omega_p^2 = 4\pi Ne^2/m^*$ is the square of the plasma frequency with N the number of free electrons per unit volume, m^* is the effective mass, and τ is the electron scattering time. Section V contains a discussion of the results, with a summary and concluding remarks in Sec. VI.

II. EXPERIMENTAL METHODS

The Hg-chain salts for this study were synthesized and crystals grown by two different methods. Large single crystals of $Hg_{2.86}AsF_6$ were grown

from a mercury surface in contact with a solution of $Hg_3(AsF_6)_2$ in liquid sulfur dioxide (SO_2) as described by Gillespie and Cutforth,[5] or from a mercury surface in contact with a solution of arsenic pentafluoride (AsF_5) in liquid SO_2 at room temperature.[6]

Neutron-diffraction studies of single crystals prepared by the two different techniques were carried out by Williams and Schultz[6] confirming the earlier x-ray results obtained for $Hg_{2.86}AsF_6$ by Brown *et al.*[2] The diffuse planes (periodicity of 2.64 Å) were observed for crystals of both materials; other crystallographic data are also in precise agreement with the x-ray results reported for $Hg_{2.86}AsF_6$.

The crystals used for the optical studies were well faceted, silvery-golden in appearance, with dimensions as large as $25 \times 25 \times 2$ mm. Well defined faces were flat or gently curved and specular; light reflected brightly and images could be seen. The larger area flat faces showed isotropic reflection when viewed through a polarizer and were thus identified as coincident with the crystallographic $\vec{a}$-$\vec{b}$ plane. Perpendicular edge faces went from bright gold with $\vec{E}$ parallel to the $\vec{a}$-$\vec{b}$ plane to dull blue for $\vec{E}$ parallel to $\vec{c}$.

A Beckman DK-2 spectrophotometer with a drop-in double beam reflectance attachment was used for all measurements.[7] Studies at room temperature were carried out on crystals in the evacuated Pyrex reaction bulb (blown from Pyrex, 1 mm thick) in which the crystal was grown. Under such conditions the crystals appear to be stable indefinitely. As a check at room temperature and to obtain data at low temperatures, crystals were transferred in a controlled atmosphere (argon) dry-box into a specially constructed[8] sealed cell with a sapphire window. The crystals were cocked at a slight angle with respect to the sapphire window to avoid reflection of light from the window. After removal from the dry box, the encapsulated crystals were stable over a period of a few days. Quantitative corrections of light loss from the window were obtained by comparison to an aluminum mirror similarly mounted behind a piece of sapphire. For low-temperature studies the sapphire window cell was attached to the cold finger of an Air Products Helitron. The temperature of the cold finger was monitored with a thermocouple.

To correct for any light loss due to slight curvature of the reflecting surface a separate measurement of the absolute reflectance was made at room temperature. A selenium or silicon photovoltaic cell (area of $\sim\frac{1}{3}$ in.^{2}) was placed at the surface of the bulb approximately 2 in. from the crystal-reflecting surface. To obtain the normalization the bulb was then rotated to move the crystal out of the beam, and the detector was moved to collect the light after it had passed through the bulb. These measurements were repeated at several fixed wavelengths in the spectral range 1.1–1.6 eV(Si) and 1.95–2.15 eV(Se). Analysis of the geometrical optics together with visual observation of the image of the slit before and after reflection from the crystal surface provided convincing evidence that the photovoltaic detector was picking up more than 95% of the true reflected light.

Measurements of the edge facets were carried out on crystals in the reaction bulb using polarized light. To obtain the angle of the edge faces with respect to the $\vec{a}$-$\vec{b}$ plane, beams of light were followed in and out of the bulb on polar graph paper; the corresponding angles are accurate to about ±4°.

III. EXPERIMENTAL RESULTS

A. Normal-incidence spectrum of the isotropic face ($\vec{a}$-$\vec{b}$ plane)

The reflectance spectrum of the isotropic face of a single crystal of $Hg_{2.86}AsF_6$ is shown in Fig. 1. The absolute value of the reflectance is uncertain to about 2%. The relative accuracy, one frequency to another as determined from reproducibility of different scans, is approximately 2% between 0.5 and 4.2 eV.

The dominant feature in the $\vec{a}$-$\vec{b}$ plane reflectance is the edge near 2.7 eV with the rapid rise to metal-like values at lower frequencies. The general shape is consistent with a plasma edge expected from Eq. (1) when the frequency is increased from $\omega < \omega_p/(\epsilon_\infty)^{1/2}$ to $\omega > \omega_p/(\epsilon_\infty)^{1/2}$. The minimum reflectance occurs at 3.7 ± 0.1 eV with a value of approximately $\frac{1}{3}$%. As anticipated from the tetragonal crystal symmetry,[2] any anisotropy in $\mathcal{R}$ in the a-b plane at 2 eV was unobservable with no detectable shift in plasma edge location at different angles of the polarizer.

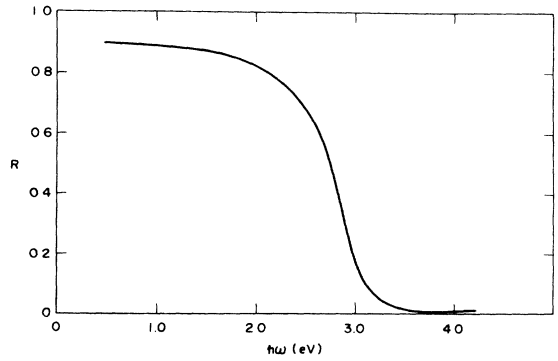

FIG. 1. Normal incidence reflectance of the isotropic crystal face ($\vec{a}$-$\vec{b}$ plane) at room temperature.

Figure 2 shows the $\vec{a}$-$\vec{b}$ plane reflectance edge at selected temperatures from room temperature down to approximately 25 ± 15 K; temperatures are indicated in Fig. 2. The uncertainty in the quoted lowest temperature arises from the use of argon exchange gas as required by mounting the sample in the controlled atmosphere dry box. Above 50 K, the temperature should be accurately given by the thermocouple on the cold finger. No qualitative changes were noted in the low-temperature spectrum although the curves do bend more sharply consistent with an increased scattering time. The changes in parameters are relatively small and will be discussed in connection with the Drude fits.

B. Normal-incidence spectrum of the anisotropic faces

The polarized reflectance spectrum of anisotropic faces of single crystals of $Hg_{2.86}AsF_6$ are shown in Fig. 3. The different faces are labeled according to the measured angle as defined in the inset to Fig. 3; $\varphi = 0$ corresponds to reflection from the $\vec{a}$-$\vec{b}$ plane, $\varphi = 49°$ corresponds to reflection from the (111) plane, and $\varphi = 60°$ corresponds to reflection from the (011) plane. The raw data for $\vec{E}$ polarized in the $\vec{a}$-$\vec{b}$ plane (denoted ||) are identical in shape with the isotropic face consistent with the crystal symmetry. The || data from these smaller side facets have been normalized (to account for relative light losses, etc., of order 20%) to agree in absolute value with the results obtained from the isotropic face. The same normalization has been applied to the non-||-polarization data. The non-|| curves are known to a relative accuracy of 3%. The anisotropy at 1.5 eV is approximately 10 to 1 and checked to be $\cos^2\theta$, where θ is the angle between the polarization vector and the $\vec{a}$-$\vec{b}$ plane.

We emphasize that the data shown in Fig. 3 are

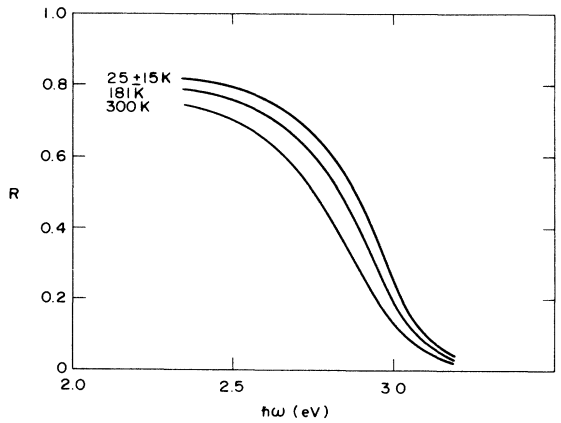

FIG. 2. Temperature dependence of the normal incidence reflectance from the $\vec{a}$-$\vec{b}$ plane.

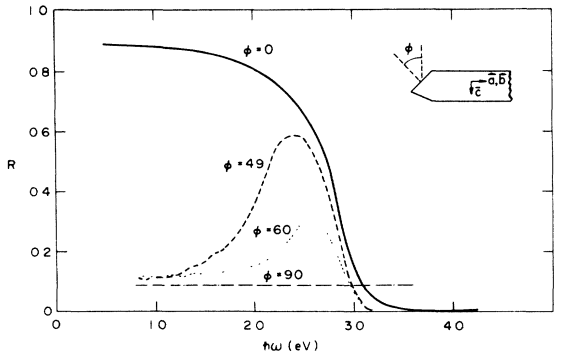

FIG. 3. Normal incidence reflectance of the anisotropic faces. The angle φ is defined in the inset.

normal-incidence reflectance curves from planes at an angle φ with respect to the principal $\vec{a}$-$\vec{b}$ plane. The results are analyzed in detail in Sec. IV. The non-|| curve for $\varphi = 90$ corresponds to light polarized along the crystallographic $\vec{c}$ direction, i.e., perpendicular to both sets of chains. The reflectance for $\vec{E} \parallel \vec{c}$ is flat and featureless (any variations were less than about 2% of $\mathcal{R} = 1$) with no sign of a metallic reflection edge in the frequency range studied.

IV. ANALYSIS OF RESULTS

Figure 4 shows a fit (dashed curve) to the $\vec{a}$-$\vec{b}$ plane reflectance (solid curve) using the Drude dielectric function [Eq. (1a)] in the Fresnel equation for normal incidence reflectance

$$\mathcal{R} = \frac{|\epsilon| + 1 - [2(|\epsilon| + \epsilon_1)]^{1/2}}{|\epsilon| + 1 + [2(|\epsilon| + \epsilon_1)]^{1/2}}, \tag{2}$$

where $\epsilon = \epsilon_1 + i\epsilon_2$. To obtain the dashed curve a least-squares fit was carried out arbitrarily restricting the input data to the range 1.3 to 4.2 eV. The experimental curve in Fig. 4 represents the

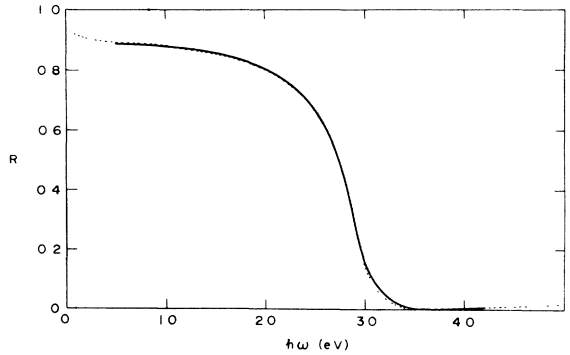

FIG. 4. Drude fit (dashed line) to the $\vec{a}$-$\vec{b}$ face reflectance (solid line). The experimental curve represents the raw data from Fig. 1 with a uniform $\frac{1}{3}$% subtracted.

raw data from Fig. 1 with a uniform $\frac{1}{3}\%$ subtracted to correct for scattered light and residual non-Drude ϵ_2 as discussed below. The free parameters were ω_p, ϵ_∞, and τ since the absolute reflectance was determined using the wide-angle photovoltaic detector as described above. Trial fits with a 1% change in reflectance gave only small changes in parameters. The results are summarized in Table I.

The values listed in Table I are our best estimate of the Drude parameters based on a least-squares fit ($\chi^2 = 6 \times 10^{-5}$) to the simple model. By systematically varying the input parameters, we have concluded that $\hbar\omega_p = 4.82 \pm 0.6$ eV, $\epsilon_\infty = 2.70 \pm 0.55$, $\hbar/\tau = 0.27 \pm 0.01$ eV, and $\hbar\omega_p/\epsilon_\infty^{1/2} = 2.93 \pm 0.03$ eV. The error limits were determined from fits with χ^2 double the minimum value. An independent relation between ω_p and ϵ_∞ can be obtained from the frequency at which minimum reflectance occurred; $\omega_p^2/(\epsilon_\infty - 1) = \omega_{\min}^2$. Using the experimental value of $\hbar\omega_{\min} = 3.7 \pm 0.1$ eV and $\hbar\omega_p/\epsilon_\infty = 2.93 \pm 0.03$ yields $\epsilon_\infty = 2.66 \pm 0.2$ and $\hbar\omega_p = 4.8 \pm 0.3$ eV. Attempts at more extensive fits (multiple plasma edges, inclusion of an energy gap, additional Lorentzian oscillators, etc.) do not appear warranted at this time. Moreover, as discussed below, these parameters are sufficient to quantitatively explain the anisotropic reflectance shown in Fig. 3.

The values for ω_p and τ can be used to obtain a measure of the optical conductivity through the standard relation

$$\sigma_{\text{opt}} = (1/4\pi)\omega_p^2 \tau . \tag{3}$$

Using $\hbar\omega_p = 4.8$ eV and $\hbar/\tau = 0.27$ eV ($\tau = 2.3 \times 10^{-15}$ sec) leads to $\sigma_{\text{opt}} = 1.2 \times 10^4$ $(\Omega\,\text{cm})^{-1}$ to be compared with the room-temperature dc and contactless ac (100-kHz) values of 10^4 $(\Omega\,\text{cm})^{-1}$.[1,9,10] The excellent agreement provides some justification of the simple Drude approach.

The temperature-dependent plasma edge parameters were obtained from analysis of the data of Fig. 2 ($T = 302$, 181, and 25 ± 15 K) together with corresponding curves obtained at $T = 241$, 120, 90, and 50 K. In each case, least-squares Drude fits were generated (with fixed $\epsilon_\infty = 2.7$) using ω_p, τ, and the absolute normalization as free parameters. The data of Fig. 2 are plotted using the absolute normalization (in the range 0.8–1.0) as determined from the Drude fits. The results are summarized

TABLE I. Drude parameters (300 K).

$\hbar\omega_p = 4.82 \pm 0.6$ eV
$\hbar/\tau = 0.27 \pm 0.01$ eV
$\epsilon_\infty = 2.70 \pm 0.55$
$\hbar\omega_p/\epsilon_\infty^{1/2} = 2.93 \pm 0.03$

TABLE II. Drude parameters at selected temperatures.

Temperature (K)	$\hbar\omega_p$ (eV)	$\hbar/\tau$ (eV)
301	4.75	0.229
241	4.80	0.208
181	4.82	0.194
120	4.83	0.199
90	4.84	0.208
55 ± 5	4.83	0.188
25 ± 15	4.87	0.174

in Table II and plotted in Figs. 5(a) and 5(b). The results summarized in Tables I and II were obtained from two independent crystals grown separately. The difference in $\hbar\omega_p$ is well within the absolute uncertainty. The somewhat larger value for τ in Table II may indicate a more-nearly-perfect crystal.

The overall change in $\hbar\omega_p$ on going to low temperature [Fig. 5(a)] is a blue shift of approximately 2% consistent with a small volume thermal contraction of the sample. The change in $\hbar/\tau$ is somewhat larger (~15%) as shown in Fig. 5(b). The solid line in Fig. 5(b) is drawn with slope k_B for comparison. A linear temperature dependence with slope k_B would be expected from simple electron-phonon scattering with coupling constant $\lambda \simeq 1$.[11]

Analysis of the anisotropy data summarized in Fig. 3 requires a treatment of normal incidence reflectance from a plane which is not coincident with the principal optical axes of the solid.[12] For

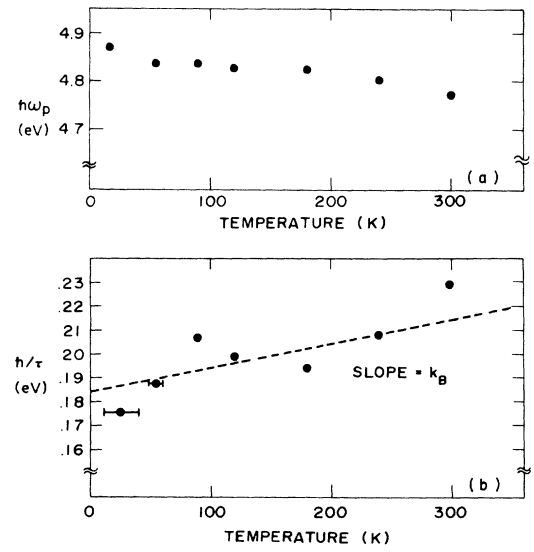

FIG. 5. (a) Temperature dependence of the plasma frequency. (b) Temperature dependence of $\hbar/\tau$.

a uniaxial (tetragonal) crystal, we define the dielectric tensor

$$\vec{\epsilon} = \begin{pmatrix} \epsilon_{ab} & 0 & 0 \\ 0 & \epsilon_{ab} & 0 \\ 0 & 0 & \epsilon_c \end{pmatrix}, \tag{4}$$

where $\epsilon_{ab} = \epsilon_\infty - \omega_p^2/(\omega^2 + i\omega/\tau)$ corresponds to the dielectric function along the chains and $\epsilon_c = \epsilon_\infty$ corresponds to the assumed constant perpendicular value. Defining the vector index of refraction

$$\vec{k} = (\omega/c)\vec{n}\,, \tag{5}$$

it is straightforward to show that there are two independent solutions:

$$\text{(i) } n^2 = \epsilon_{ab}: \tag{6}$$

This is the ordinary wave in which the incident light is polarized in the *ab* plane (i.e., along a principal "metallic" direction);

$$\text{(ii) } n_z^2/\epsilon_{ab} + (n_x^2 + n_y^2)/\epsilon_c = 1: \tag{7}$$

This is the extraordinary wave for which the velocity of propagation depends on direction.

For the case of normal incidence where the optical axis makes an angle φ from the normal (see Fig. 3), Eq. (7) reduces to

$$n^2(\cos^2\varphi/\epsilon_{ab} + \sin^2\varphi/\epsilon_c) = 1\,. \tag{8}$$

Equation (8) can be used to determine $n(\varphi)$ and thus the reflectance through the standard relation

$$\mathcal{R}_{(\varphi,\omega)} = \left|(n_{(\varphi,\omega)} - 1)/(n_{(\varphi,\omega)} + 1)\right|^2, \tag{9}$$

where, in the present case, $n_{(\varphi,\omega)}$ is complex due to the Drude form of ϵ_{ab}. The theoretical results for $\mathcal{R}_{(\varphi,\omega)}$ are shown in Fig. 6 using the parameters from Table I for ω_p, ϵ_∞, and τ. Figure 6 presents a direct comparison of the theoretical curves to the data with *no additional parameters*. The overall good qualitative and quantitative agreement provides additional confirmation of the validity of the simple one-dimensional Drude treatment of this anisotropic metal.

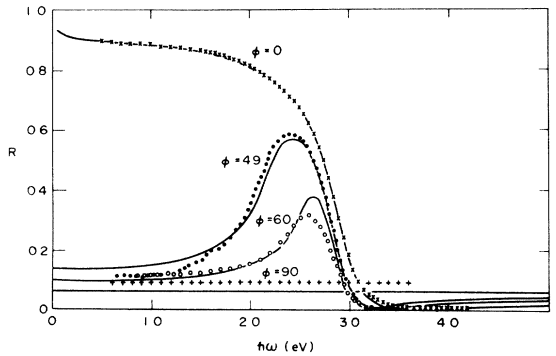

FIG. 6. Normal incidence reflectance of the anisotropic faces; the angle φ is defined in Fig. 3. The solid curves are calculated from Eqs. (7), (8), and (9) using the parameters in Table I. There are no additional parameters.

Only an upper limit can be placed on the magnitude of the perpendicular ($\vec{E} \parallel \vec{c}$) optical conductivity. Since no plasma edge or decrease in reflectance is observed over an extended range out to 0.5 eV one can conclude that $\omega_p^c < 0.5$ eV. Thus assuming equal scattering times, we have

$$\sigma_{\text{opt}}^c/\sigma_{\text{opt}}^{ab} = (\omega_p^c)^2/(\omega_p^{ab})^2 \leq 10^2\,,$$

in agreement with the observed electrical anisotropy ($\sigma_c/\sigma_{ab} \simeq 10^{-2}$) obtained from dc measurements.[1,9,10]

V. DISCUSSION

The value of $\hbar\omega_p$ obtained from the Drude fit can be used to estimate the optical effective mass m^*. Liquid-Hg calculations of electronic properties typically assign two electrons per atom, consistent with the $6s^2$ atomic configuration, in a nearly-free-electron band. The absence of structure in the reflection spectra described above at energies above the plasma edge (contrast with Ag and the transition metals) together with the relatively small core dielectric constant ($\epsilon_\infty = 2.7$) suggest few strong transitions and a simple band structure in this energy range. Moreover, the very small Hg-Hg distance along the chain (2.64 Å as compared with 3.0 Å in Hg metal) suggests that free-electron theory is a reasonable starting approximation.

The optical and electronic properties of this novel metallic system are evidently dominated by the Hg-chain structure. The structural data from the crystallographic studies[2,6] yields (approximately) three Hg atoms per chain in the unit cell and two chains per unit cell ($a = b = 7.54$ Å, $c = 12.34$ Å) for a particular polarization direction. Assuming the $(AsF_6)^-$ anion is fully ionic, one electron is charge transferred from the band, for every six; and there are five electrons per chain in the unit cell. Thus, for calculation of ω_p in the *a-b* plane, the appropriate electron density is $N \simeq 10$ electrons/unit cell $= 1.42 \times 10^{22}$ cm^{-3}, and the resulting value for ω_p is given by

$$\hbar\omega_p = 4.43(m/m^*)^{1/2}\ \text{eV}\,. \tag{10}$$

Comparison with the experimental value (Table I), $\hbar\omega_p^{\text{expt}} = 4.8 \pm 0.3$ eV yields $m^* \cong m$. Within the experimental uncertainty, the optical mass is approximately equal to the free-electron value.

Assuming, therefore, a free-electron picture for electronic motion along the chain arising from the strong overlap between Hg-Hg wave functions at a spacing of $\tilde{a} = 2.64$ Å with approximately $\frac{5}{6}$

electron per atom, one obtains the band structure shown in Fig. 7. The relevant parameters are as follows: the Fermi energy, $E_F = 3.75$ eV; the Fermi momentum, $k_F = \frac{5}{6}(\pi/2.64) \times 10^8$, and the Fermi velocity $v_F = 2 \times 10^8$ cm/sec. From the optical-scattering time (Table I), we obtain a mean free path $l = v_F\tau \simeq 50$ Å at room temperature, approximately 20 Hg-Hg spacings. Within this picture a weak interband transition might be expected at E_{ib} as shown in Fig. 7 where $E_{ib} \sim 3.6$ eV. Such an interband transition may contribute to the minimum reflectance in the range 3.5–4 eV.

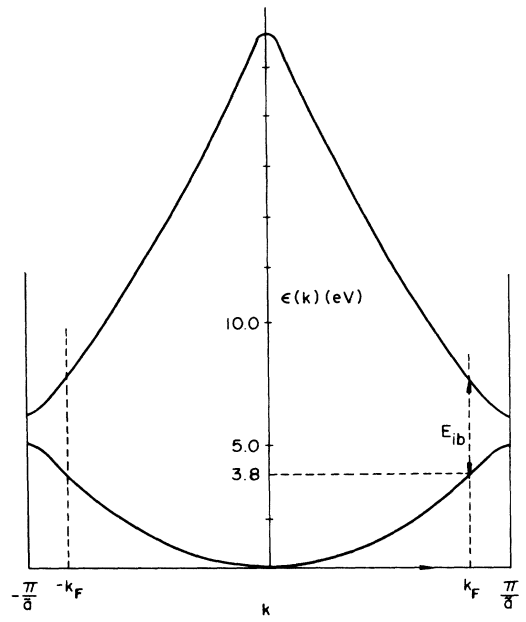

FIG. 7. Schematic diagram of the electronic band structure of $Hg_{2.86}AsF_6$ along the chain direction (see text).

VI. SUMMARY AND CONCLUSION

In this study we have measured the polarized reflectance from single-crystal faces of the anisotropic Hg-chain conductor $Hg_{2.86}AsF_6$. The results indicate metallic behavior for electronic excitations along the chains (in the a-b plane) with free-electron Drude theory giving a satisfactory initial description of the data.

Normal incidence studies of reflectance from crystal faces at an angle with the a-b plane have been analyzed to provide a description of the complex dielectric tensor in the spectral range from 0.5 to 4.2 eV. The results confirm the validity of the simple treatment of these anisotropic conductors as consisting of quasi-one-dimensional metallic chains. Extension of the results into the infrared and far infrared is required to clarify the importance of interchain coupling. We note, however, that although the dc conductivity is anisotropic, the conductivity along the $\vec{c}$ axis at low temperatures exceeds 10^5 $(\Omega\,\mathrm{cm})^{-1}$,[10] so that a picture of weakly coupled one-dimensional chains is perhaps oversimplified.

The additional incommensurate periodicity infrared from the observation of the diffuse streaks is suggestive of similar structural features observed in[3] TTF-TCNQ and[4] KCP resulting from the Peierls instability. The optical experiments reported here show no evidence of an energy gap in the excitation spectrum with magnitude greater than approximately 0.5 eV. However, extension to longer wavelengths is clearly required to investigate the possibility of a Peierls gap in the excitation spectrum.

ACKNOWLEDGMENTS

We thank Dr. J. Williams and Dr. A. Schultz of Argonne National Laboratory for their cooperation on the neutron-diffraction crystallographic study of the compounds studied in this paper and for many helpful and important discussions.

---

*Work supported by the NSF MRL Program under Grant No. DMR 76-00678. The synthesis, crystal growth, and chemical studies were supported in part by the NSF through Grant No. MPS 73-04771-A1.

[1]B. D. Cutforth, Ph.D. thesis (McMaster University, Hamilton, Ontario, 1975) (unpublished); B. D. Cutforth, W. R. Datars, R. J. Gillespie, and A. van Schyndel, Adv. Chem. Ser. 150, 147 (1976).

[2]I. D. Brown, B. D. Cutforth, C. G. Davies, R. J. Gillespie, P. R. Ireland, and J. E. Vekris, Can. J. Chem. 52, 791 (1974).

[3]*Low Dimensional Cooperative Phenomena,* edited by H. J. Keller (Plenum, New York, 1975); *Lecture Notes in Physics 34: One-Dimensional Conductors* (Springer, New York, 1975).

[4]*Chemistry and Physics of One-Dimensional Metals,* edited by H. J. Keller (Plenum, New York, 1977).

[5]R. J. Gillespie and B. D. Cutforth (private communication).

[6]N. D. Miro, A. G. MacDiarmid, A. J. Heeger, A. F. Garito, C. K. Chiang, A. J. Schultz, and J. M. Williams (unpublished). Under certain growth conditions an adduct of composition $Hg_{2.86}AsF_6 \cdot yAsF_3$ $(0 < y < 1)$ is obtained. However, neutron-diffraction studies show

identical crystal structures with no sign of AsF_3, and electrical and optical properties indistinguishable from those of $Hg_{2.86}AsF_6$. Evidently the AsF_3 reaction product is physically entrained or occluded in such crystals during growth.

[7]A. A. Bright, A. F. Garito, and A. J. Heeger, Phys. Rev. B 10, 1328 (1974). The measurements from 1.3 to 4.2 eV utilized the spectrophotometer as a double-beam instrument. Additional measurements from 0.5 to 2.5 eV used an external PbS detector in a method similar to the absolute measurements in the text.

[8]We thank Professor J. Fischer for providing us with the sealed optical cell.

[9]W. R. Datars, B. D. Cutforth, A. van Schyndel, and R. J. Gillespie, Bull. Am. Phys. Soc. 20, 439 (1975); Solid State Commun. 21, 377 (1976); E. S. Koteles, W. R. Datars, B. D. Cutforth, and R. J. Gillespie, *ibid*. 20, 1129 (1976).

[10]C. K. Chiang, R. Spal, A. Denenstein, A. J. Heeger, N. Miro, and A. G. MacDiarmid, Solid State Commun. 22, 293 (1977).

[11]J. J. Hopfield, Comments Solid State Phys. 3, 48 (1970).

[12]F. Wooten, *Optical Properties of Solids* (Academic, New York, 1972).